



Moisture Detector in Concrete Using Convolutional Neural Networks

Silva, J. G. G.¹, Araújo, T. M.¹, Maia, E. H. B.¹, Francês, C. R. L.²

¹Computing Dept. (DECOM), CEFET-MG

Álvares de Azevedo St. 400, Bela Vista - Divinópolis-MG - Brazil - 35503-822

joaogu.2001@gmail.com, thabatta@cefetmg.br, habib@cefetmg.br

²Technology Innovation Agency, UFPA

renato.frances2010@gmail.com

Abstract

Concrete can deteriorate in different ways, such as pH changes, compressive strength reduction, and microbe growth, all associated with moisture. As a result, hazardous installations could be damaged entailing financial, human, and environmental losses. Infrared thermography and visual inspection are mainly used for detecting moisture in edifications but lack significant prices and real-time surveillance. Otherwise, computational methods combine real-time, custom, and affordable evaluation, becoming feasible. The research develops a CNN architecture for classifying moistened concrete, with a low-complexity combination of hyperparameters. However, computational vision and neural networks suffer from the absence of public structural damage databases with enough images. Therefore, this study obtained images of concrete surfaces from urban edifications by mobile devices. Furthermore, the Neural Networks is purposely built for binary classification, becoming assisted by pictures for recognizing moisture in concrete surfaces. CNN scored an AUC-ROC of 0.94, achieving excellence in distinguishing the "wet" and "dry" classes. It enables the identification of long-time moisture and, thus strength loss in concrete. Nevertheless, the research provides humidity indicators to classify building surfaces. This knowledge can be used to mitigate disasters such as leaks in dams and nuclear reactors, preventing natural disasters.

Keywords: Concrete, Model, Moisture, Neural, Convolutional.

1 Introduction

Several researches have shown moisture in concrete as a building pathology[1] since it changes its mechanical properties [2][3]. After being moistened, the material should pass chemical reactions like Steel reinforcement corrosion[4], alkali-aggregate reaction[5], and moisture gradient. Then the deterioration of concrete caused by these reactions affects radar signals passing through it[6], cracks it exacerbating other deterioration mechanisms[7], and decreases the concrete resistance to bending moments[8][9]. Furthermore, referenced chemical reactions lead to broad kinds of disasters in Hazardous installations such as NPP[10], Dams[11], and Hydroelectric[12]. For this reason, tracking moisture in concrete surfaces prevents risks such as human losses and ecosystem impact. In essence, moisture is a risky factor when found above concrete surfaces, on the other hand, machine learning with feature engineering[13], identifies wet surfaces by tracking seepage, mold and other damp indicators. However, classifying moistened concrete surfaces with computational methods enhances security through a tough but achievable approach[14][15].

2 Methodology

The Convolutional Neural Network is developed and enhanced in four stages (a) Data Acquisition and Processing, (b) Environment Setup, and (c) CNN architecture and Design.

2.1 Data Acquisition and Processing

Researchers and engineers in the field of civil engineering have already demonstrated the strength and innovative capacity of brought about by SHM through Convolutional Neural Networks[16][17][18]. Promoting a far filed

vision based data acquisition, and digital pattern of sampling facilitate the acquisition and processing of large sets of data[19]. Otherwise dampness inspection of concrete use to be realized by sensors[20], on-site inspections[21], and laboratory tests [22](Measurements), methods that do not benefit from sampling in the same way. In view of the advantages described under the use of CNNs for SHM the initial step in the construction of the model is defining the image dataset, in the study it is composed of 1.854 samples captured by 3 different cameras(MP is a measurement based on how many 10^6 pixels resolution is defined, and $f/$ is the f-number which is conceived by the division between the system's focal length and diameter of entrance pupil):

Table 1. Smartphone Cameras For Sampling, with or without pixel binning[23] and OIS[24]

Smartphone	Resolution(MP)	Aperture($f/$)	pixel binning(True/False)	OIS(True/False)
Xiomi Redmi 10C	50	1.8	True	False
Samsung Galaxy A14	50	1.8	True	False
Apple iPhone 12 Pro	12	1.6	False	True

After capturing the datasets, the next stage was to apply labeling process, which involved depict presence or absence of visible moisture on the surface of concrete. Moreover all images. Thereafter, Images were randomly distributed in a respective proportion(Table 3) in Train, Validation, and Test directories feeding into a CNN to build a binary classifier that can distinguish between 'wet' (negative output, probability close to 0) or 'dry' (positive output, close to 1).

Table 2. Sample Division

Classes	Directories					
	Train		Validation		Test	
	Images	(%)	Images	(%)	Images	(%)
Wet	733	39.54	97	5.23	109	5.88
Dry	709	38.24	97	5.23	109	5.88
Total	1442	77.78	194	10.46	218	11.76

To feed the model and start the training resolution and pixel color of each image were normalized. Since the lower variance of pixel values is achieved, inherent characteristics of images could be better represented, and noisy factors like light could be reduced[25]. In accordance, images were resized to 128x128 pixels, following proposed low complexity architecture in page 24 of [16].

2.2 Environment Setup

Before build the model, is essential to prepare an ambience that is equivalent to the one used for that research. This methodology allows to replicate the model and experiments done.

- Hardware: 8GB de RAM Intel(R) Core(TM) i5-3470 CPU @ 3.20GHz 3.20 GHz
- Operational System: Windows 10 64-bit
- Programming Language: Python 3.9.11
- Modules: Numpy 1.24.3, Scikit-learn 1.5.0, Keras 2.13.1, Tensor-Flow 2.13.1, Pandas 2.2.2, Matplotlib 3.9.0, seaborn 0.13.2, cv2 4.9.0, PIL 10.3.0.
- IDEs: Jupyter-Notebook, Google Colaboratory and Visual Studio Code.

2.3 CNN Architecture and Design

The suggested architecture of CNN developed is detailed in (Table 4). and initially addressed Detection of Geotechnical Damage. Nevertheless The structure of classifier is based on 3 Convolutional Layers[26], both have 32 filters of resolution equals to 3, and each one of them sends the output to a ReLu(eq. 1) next passing their values



Figure 1. 6th wet sample



Figure 2. 225th wet sample



Figure 3. 392th wet sample



Figure 4. 4th dry sample

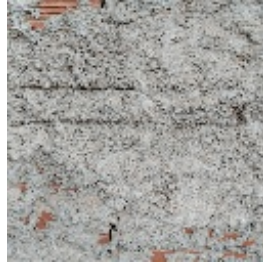


Figure 5. 197th dry sample

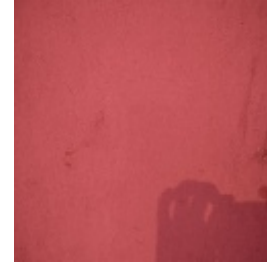


Figure 6. 478th dry sample

to 2x2 max-pooling2D operator[27]. Then just the second and the third ones had a Dropout[28] of 0.25 applied on their respective outputs. Finally, a flatten layers is placed after the Dropout at third layer, flatten operator converts a 3 channel matrix with width and heigh(Tridimensional Tensor) in an Unidimensional Tensor. Afterward is added two Dense layers activated by ReLu with 128 units, followed by 1 neuron with sigmoid activation(which is described by $\sigma(x) = \frac{1}{1+e^x}$). The training phase of best model is done across 2000 epochs saving a weight file every 10 epochs.

$$ReLU(x) = \begin{cases} x & \text{if } x \geq 0 \\ 0 & \text{if } x < 0 \end{cases} \quad (1)$$

Table 3. Network Architecture and respective Hyperparameters of each opeator

Kind	Parameters
Convolutional 32F 3x3	ReLU, Max-Pooling 2D (2x2)
Convolutional 32F 3x3	ReLU, Max-Pooling 2D (2x2), Dropout (25%)
Convolutional 32F 3x3	ReLU, Max-Pooling 2D (2x2), Dropout (25%)
Fully Connected Layer	Flatten, ReLU (128 units), ReLU (128 units), σ (1 unit)

Before Vizualize the Model is important to improve the concern of what is a Dense Layer and how each unit works. A single neuron(n) or unit output(y^n) can be abstracted using tree operations.First the input tensor from Flatten(x_i with D elements) is linear combined with a tensor(w_i):

$$\sum_{i=1}^D x_i \cdot w_i \quad (2)$$

Remark 1: Initial Weights choice. The weights of model were intialized with Xavier uniform initialization or Normalized Initialization in [29](Equation 16) and Keras documentation[30] once the study is using Keras 2.13 for make Dense layers[31] and its utility can be comprehended at the conclusion of the explanation of the dense layer.

Subsequently the bias is added into the result:

$$\left(\sum_{i=1}^D x_i \cdot w_i \right) + b \quad (3)$$

Remark 2: Initial Bias choice. All bias are initialized as 0 following the method of Katanforoosh & Kunin, "Initializing neural networks", deeplearning.ai, 2019[32]. once the study is using Keras 2.13 for make Dense layers. And Third the result serves as the input set for the activation function, which is ReLu at neurons in both first twice Dense layers, and a unique sigmoid at last:

$$y^n = ReLu\left(\sum_{i=1}^D x_i \cdot w_i\right) + b \quad (4)$$

Finally the Dense layers or neural network [33] in our model is structured as an input layer of neurons($l1$), one hidden layers of neurons($l2$), and a final unique neuron. Read y^l as output of a layer. eq. (5) define output of layer 1, then eq. (6) output of layer 2 and finally eq. (7) output of layer 3:

$$y^{l1} = ReLu\left(\sum_{i=1}^D x_i \cdot w_i^{l1}\right) \quad (5)$$

$$y^{l2} = ReLu\left(\sum_{i=1}^D y_i^{l1} \cdot w_i^{l2}\right) + b_2 \quad (6)$$

$$y^{l3} = \sigma\left(\sum_{i=1}^D y_i^{l2} \cdot w_i^{l3}\right) + b_3 \quad (7)$$

Remark 3: Brief about Dense Neural Networks. The term is used Dense to describe that each neuron is connected to every neuron on previous layer.

3 Results

Given design reach optimal metrics of classification on their first 900 epochs. For a 0.877976 threshold, the Confusion Matrix in Figure 7 is earned. Afterwards, testing phase evaluate the model with metrics like: precision or P (i.e. ratio of correct wet concrete predictions about all wet concrete predictions), recall or R (means ratio of true wet concrete predictions to the correct predicted wet instances summed to false dry concrete predictions, i.e. an ability to identify all actual wet instances), f1-score or F_1 (a balance score that considers both recall and precision):

Table 4. Classification metrics about test dataset

class	P	R	F_1	support
dry	0.94	0.94	0.94	109
wet	0.94	0.94	0.94	109

Furthermore, Receiver Operating Characteristic(ROC) consider a proportion of all correct predictions to be defined, with more accurate measure of classifier performance[34]. An alternative to score efficiency of classifier is use Area Under ROC(ROC-AUC)[35] as a scalar that define how much it is right on their ratings. Tests dimensioned model ROC-AUC of this study on Figure 8:

Since the model follows a balanced distribution on the test sample, WAUC(Weighted AUC) or Multi-class AUC [36] achieve the same value as AUC in eq. (9):

$$w_{dry} = \frac{\text{Total test dry samples}}{\text{Total test samples}} \quad w_{wet} = \frac{\text{Total test wet samples}}{\text{Total test samples}} \quad (8)$$

$$WAUC = P_{dry} \times w_{dry} + P_{wet} \times w_{wet} \equiv WAUC = 0.94 * 0.5 + 0.94 * 0.5 \equiv WAUC = AUC \quad (9)$$

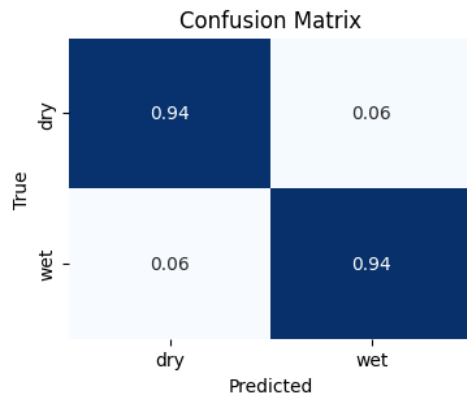


Figure 7. Confusion Matrix

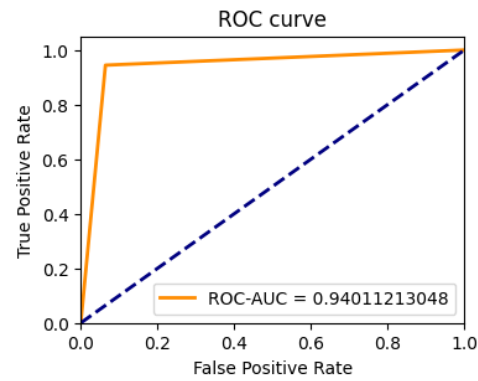


Figure 8. AUC-ROC Graphic

4 Conclusions

A Moisture Detector in Concrete using Convolutional Neural Networks was proposed. To reach it, images were collected with different mobile cellphones, then divided respectively into training, validation, and test samples, afterwards the sets were processed to assume 128x128 pixels of resolution, forming datasets used to develop the Moisture Detector. The features captured cover the action of moisture over a long time, like mold, internal leakage, and even remnants of alkali-aggregate reaction. After training, classifications of the model raise good metrics mainly about ROC-AUC and WAUC (which are equal to 0.94). Further work would perform better to realize distinguishment with the absence or presence of humidity in patterns such as images with different shades of white airbrushed on top of each other, dry masonry walls, white mold distributed in light shades of blue, and texture similar to granilite concrete.

Acknowledgements. The authors would like to thank the support by the Coordination for the Improvement of Higher Education Personnel (CAPES), the National Council for Scientific and Technological Development (CNPq) and Institutional Program for Research Promotion of PROMEQ-CEFET-MG.

Authorship statement. This Article uses Contributors Role Taxonomy (CRediT):

- Araújo, T. M.: Conceptualization, Methodology, Software, Validation, Formal analysis, Investigation, Review & Editing, Supervision, Project administration and Funding Acquisition.
- Francês, C. R. L.: Conceptualization.
- Maia, E. H. B.: Project administration and Funding acquisition.
- Silva, J. G. G.: Software, Validation, Formal analysis, Investigation, Writing, Review & Editing, Supervision, Project administration, Funding acquisition.

References

- [1] WATT, D. Building Pathology Principles and Practice Second Edition. 2nd ed. ed. [s.l.] Blackwell Publishing Ltd , 2007.
- [2] SHOUKRY, S. N. et al. Effect of moisture and temperature on the mechanical properties of concrete. Construction and Building Materials, v. 25, n. 02, p. 688–696, 21 ago. 2010.
- [3] ASTM. Standard Test Method for Obtaining and Testing Drilled Cores and Sawed Beams of Concrete. <https://www.astm.org/c0042.c0042m-20.html>. Acesso em: 4 Jun. 2024. (par. 4)
- [4] HUGENSCHMIDT, J.; LOSER, R. Detection of chlorides and moisture in concrete structures with ground penetrating radar. Materials and Structures, v. 41, n. 4, p. 785, 4 Jul. 2007.
- [5] DENT GLASSER, L. S.; KATAOKA, N. The chemistry of “alkali-aggregate” reaction. Cement and Concrete Research, v. 11, n. 1, p. 1, 1 Jan. 1981.
- [6] MEHDI SBARTAÏ, Z. M. S. et al. Effect of Concrete Moisture on Radar Signal Amplitude. ACI Materials Journal, v. 103, n. 6, p. 419, 1 Nov. 2016.
- [7] FARNY, J. A.; KERKHOFF, B.; PORTLAND CEMENT ASSOCIATION. Diagnosis and Control of alkali-aggregate Reactions in Concrete. 3rd. ed. [s.l.] Portland Cement Association, 2007. p. 4
- [8] JANSSEN, D. J. Moisture in Portland Cement Concrete. <https://trid.trb.org/View/282389>. Acesso em: 4 Jun. 2024.
- [9] REINHARDT, H. W.; UNIVERSITY OF STUTTGART, GERMANY. Factors Affecting the Tensile Properties of Concrete. In: WEERHEIJM, J. (Ed.). Understanding the Tensile Properties of Concrete. [s.l.] Woodhead Publishing, 2013. p. 23.

- [10] ABDUL RASHEED, P. et al. Degradation of Concrete Structures in Nuclear Power Plants: A Review of the Major Causes and Possible Preventive Measures. *Energies*, v. 15, n. 21, p. 2–4, 28 Oct. 2022.
- [11] ZHANG, X. et al. Study on the influence of seepage field and stability of earth-rock dam with core with rainfall infiltration and drawdown of reservoir water lever. p. 1777–1781, 24 Oct. 2001.
- [12] FUNAHASHI, E. (Master), et al.. Concrete Deterioration of Dams and Hydroelectric Power Plants due to the Joint Attack of AAR/DEF – Case Studies. In: *Proceedings of the XXXIV SEMINÁRIO NACIONAL DE GRANDES BARRAGENS, 2023, Foz do Iguaçu - PR. XXXIV - SNGB - Anais*. p. 1. Accessed on: June 4, 2024.
- [13] S. Khalid, T. Khalil and S. Nasreen, "A survey of feature selection and feature extraction techniques in machine learning," 2014 Science and Information Conference, London, UK, 2014, p. 372, doi: 10.1109/SAI.2014.6918213. Accessed on: June 4, 2024.
- [14] E.T. Lima Junior, et al. "BEM Modeling of Saturated Porous Media Susceptible to Damage." *Engineering Analysis with Boundary Elements*, vol. 36, no. 2, 1 Feb. 2012, pp. 147–153, doi.org/10.1016/j.enganabound.2011.07.002. Accessed 4 June 2024.
- [15] Limão, Caio Henrique Esquina, et al. "Deep Learning Based Slope Erosion Detection." *IAES International Journal of Artificial Intelligence (IJ-AI)*, vol. 12, no. 3, 1 Sept. 2023, pp. 1428–1438, ijai.iaescore.com/index.php/IJAI/article/view/22202, https://doi.org/10.11591/ijai.v12.i3.pp1428-1438. Accessed 7 July 2024.
- [16] ALVES DE ARAÚJO, Thabatta Moreira [Araujo T]; DE MATTOS TEIXEIRA, Carlos André [Teixeira C]; LISBOA FRANCÊS, Carlos Renato [Francês C]. Enhancing geotechnical damage detection with deep learning: a convolutional neural network approach. *PeerJ Computer Science*, v. 10, p. 8, 2024. Accessed on: https://peerj.com/articles/cs-2052/
- [17] CHA, Young-Jin; CHOI, Wooram; BÜYÜKÖZTÜRK, Oral. Deep Learning-Based Crack damage Detection using convolutional neural networks. *Computer-Aided Civil and Infrastructure Engineering*, v. 32, n. 5, p. 361–378, 2017. Accessed on: https://doi.org/10.1111/mice.12263
- [18] SHI, Pengfei; FAN, Xinnan; NI, Jianjun; et al. A detection and classification approach for underwater dam cracks. *Structural Health Monitoring*, v. 15, n. 5, p. 541–554, 2016. Accessed on: https://doi.org/10.1177/1475921716651039
- [19] SWARTZ, Barbara E. The advantages of digital over analog recording techniques. *Electroencephalography and Clinical Neurophysiology*, v. 106, n. 2, p. 113–117, 1998. Accessed on: https://doi.org/10.1016/s0013-4694(97)00113-2
- [20] ALAM, Md., et al. Concrete moisture content measurement using interdigitated Near-Field sensors. *IEEE Sensors Journal*, v. 10, n. 7, Abstract, 2010. https://doi.org/10.1109/jsen.2010.2040175.1
- [21] SON, Lee How; YUEN, George C. S. Dampness in Buildings. In: *Building Maintenance Technology*. [s.l.: s.n.], 1993, p. 327. https://doi.org/10.1007/978134923150-8_14.
- [22] PARROTT, L. J. Moisture conditioning and transport properties of concrete test specimens. *Metériaux Et Constructions*, v. 27, n.8, p.461-463, 1994. Accessed on: https://doi.org/10.1007/bf02473450.]
- [23] JIN, Xiaodan; HIRAKAWA, Keigo. Analysis and processing of pixel binning for color image sensor. *EURASIP Journal on Advances in Signal Processing*, v. 2012, n. 1, 2012. https://doi.org/10.1186/1687-6180-2012-125.
- [24] LA ROSA, Fabrizio, et al. Optical Image Stabilization. [s.l.]: STMICROELECTRONICS, [s.d.], p. 3, https://www.st.com.cn/resource/en/white_paper/ois_white_paper.pdf. Acesso em: 1 Jul. 2024.
- [25] GOODFELLOW, I.; BENGIO, Y.; COURVILLE, A. *Deep Learning*. [s.l.] MIT Press, 2016. p. 327–330
- [26] ZHAO, Lei; ZHANG, Zhonglin. A improved pooling method for convolutional neural networks. *Scientific Reports*, v. 14, n. 1, 2024, p. 5. https://doi.org/10.1038/s41598-024-51258-6.
- [27] KERAS. MaxPooling2D. In: *Keras documentation. Versão 2* [s.l.]: [s.n.], 2021. https://keras.io/2.16/api/layers/pooling_layers/max_pooling2d/
- [28] SRIVASTAVA, Nitish, et al. Dropout: A Simple Way to Prevent Neural Networks from Overfitting. *Journal of Machine Learning Research*, v. 15, p. 1933, 2014. [29] GLOROT, Xavier. Understanding the difficulty of training deep feedforward neural networks. *International Conference on Artificial Intelligence and Statistics*. Chia, Sardinia, Italy: *Proceedings of Machine Learning Research*, 253, 2015. https://proceedings.mlr.press/v9/glorot10a.html.
- [30] KERAS. Layer weight initializers. In: *Keras documentation. Versão 2* [s.l.]: [s.n.], 2021. https://keras.io/2.16/api/layers/initializers/
- [31] KERAS. Dense. In: *Keras documentation. Versão 2* [s.l.]: [s.n.], 2021. https://keras.io/2.16/api/layers/core_layers/dense/
- [32] GUO, Jingru. *AI Notes: Initializing neural networks - deeplearning.ai*. deeplearning.ai, 2019. https://www.deeplearning.ai/ai-notes/initialization/index.html.
- [33] WANG, Sun-Chong. *Artificial Neural network*. In: *Springer eBooks*. [s.l.: s.n.], 2003, p. 81. https://doi.org/10.1007/97-814615-03774_5.
- [34] KOHL, Matthias. Performance Measures in Binary Classification. *International Journal of Statistics in Medical Research*, v. 1, p. 81, 2012. https://www.lifescienceglobalca.com/index.php/ijsmr/article/view/512/232.
- [35] Li, Jialiang, and Jason P. Fine. "Weighted Area under the Receiver Operating Characteristic Curve and Its Application to Gene Selection." *Journal of the Royal Statistical Society: Series c (Applied Statistics)*, 10 June 2010, p. no-no, https://doi.org/10.1111/j.1467-9876.2010.00713.x. Accessed 5 Dec. 2019.
- [36] FAWCETT, T. An introduction to ROC analysis. *Pattern Recognition Letters*, v. 27, n. 8, p. 872, 2006.